
**Separation Science and Technology**
Publication details, including instructions for authors and subscription information:
http://www.informaworld.com/smpp/title~content=t713708471

# Use of Chemical Species as Dynamic Membranes with Crossflow Microfiltration

Muhammad H. Al-Malack; G. K. Anderson

**To cite this Article** Al-Malack, Muhammad H. and Anderson, G. K.(1998) 'Use of Chemical Species as Dynamic Membranes with Crossflow Microfiltration', Separation Science and Technology, 33: 16, 2491 — 2511
**To link to this Article: DOI:** 10.1080/01496399808545315
**URL:** http://dx.doi.org/10.1080/01496399808545315

SEPARATION SCIENCE AND TECHNOLOGY, 33(16), pp. 2491–2511, 1998

# Use of Chemical Species as Dynamic Membranes with Crossflow Microfiltration

MUHAMMAD H. AL-MALACK*
KFUPM
BOX 1150, DHAHRAN 31261, SAUDI ARABIA

G. K. ANDERSON
CIVIL ENGINEERING DEPARTMENT
THE UNIVERSITY
NEWCASTLE UPON TYNE NE1 7RU, ENGLAND



## ABSTRACT

The feasibility of utilizing the phenomenon of dynamic membrane formation with crossflow microfiltration in treating domestic wastewater was investigated. The primary membrane, used throughout the investigation, was made of woven polyester. Different chemical species, such as $CaCO_3$, $FeCl_3$, and $NaAlO_2$, were used in forming dynamic membranes on top of the primary membrane. Secondary effluent from a domestic activated sludge wastewater treatment plant was treated. A calcium carbonate dynamic membrane produced a stabilized permeate flux of 90 $L/m^2 \cdot h$, with a permeate turbidity of 0.21 Nephelometric Turbidity Unit (NTU), at optimum conditions. Ferric chloride produced optimum results when it was mixed with tap water. A permeate flux and turbidity of 70 $L/m^2 \cdot h$ and 0.16 NTU, respectively, were obtained. Sodium aluminate produced a stabilized permeate flux of 77 $L/m^2 \cdot h$ when it was mixed with tap water during the formation of the dynamic membrane. The permeate turbidity was 0.16 NTU. The fouling mechanism of the three dynamic membranes was investigated, and empirical models were produced.

*Key Words.* Crossflow; Microfiltration; Dynamic membrane; Wastewater treatment; Filtration; Membrane

* To whom correspondence should be addressed. Telephone: +966 3 8604735. FAX: +966 3 8602266. E-mail: mhmalack@dpc.kfupm.edu.sa

## INTRODUCTION

Crossflow microfiltration is a process in which the formation of a filter cake is limited by a flow of the suspension tangential to the filtration medium and, because this system is pressurized, water is forced through the pores of the filter. In contrast, in the case of conventional dead-end filtration, the suspension flows at right angles to the filter medium under the applied pressure. It is clear that in the case of dead-end filtration, clogging will occur in a short time due to the build up of filtered cake, while in crossflow microfiltration, particles deposited on the filter medium are swept away by the crossflow velocity actions. Moreover, dead-end filtration is, in general, not recommended for filtration of very fine suspensions nor for the production of a very pure filtrate (1).

Due to the increasingly restrictive legal requirements, the rising costs of liquid waste disposal, and the growing need for innovative sources of water supply, liquid waste reduction, and recovery of valuable products, crossflow microfiltration processes are gaining considerable prominence in many sectors of industry.



The efficiency of crossflow microfiltration is primarily a function of the operating parameters. This efficiency is measured by the filtrate flow rate (flux) and its quality. Suspended solid concentration in the feed, temperature, crossflow velocity, transmembrane pressure, and pore size of the membrane were reported to affect the performance of crossflow microfiltration (2–4).

For evaluation of the process and economic viability of crossflow microfiltration applications, flux stability is a significant component which must be taken into consideration. Flux decay and any subsequent membrane cleaning or replacement play a key role in the overall economics of microfiltration processes. The flux decline is caused by the continuous infiltration of fine particulate matter into the concentration polarization layer or by compaction of the layer. Milisic and Bersillon (2) reported that in order to control cake formation, two types of action can be undertaken: prevent the particles from reaching the membrane or flush them out. Several techniques have been adopted to prevent the particles reaching the membrane. These include the use of abrasives, filtration aids, and electrofiltration. On the other hand, periodic backwashing, ultrasound fields, and pulsated flow are intended to remove the particles already located in the membrane or at its surface.

In crossflow microfiltration processes the formation of a secondary or dynamic membrane on top of the primary membrane occurs. Whether automatically or by design from constituents in the feed, this dynamic membrane is always formed. This phenomenon should be exploited in a beneficial way by substituting the involuntary dynamic membrane with a layer of desirable properties. Al-Malack and Anderson (5) investigated the use of $MnO_2$ as a

dynamic membrane with crossflow microfiltration in treating secondary effluent discharged from a domestic wastewater treatment plant. They reported that using dynamic membranes made of favorable materials will result in an improvement in the overall performance of the crossflow microfiltration process. The improvement in the process performance was attributed mainly to narrowing of the pore size and surface modification of the primary membrane. Holdich and Boston (6) investigated the application of dynamically formed membranes in the microfiltration of tap water, using mineral species for that purpose. These mineral species included fluorspar, diatomite, kaolin, silicate flakes, and limestone. They concluded that good permeate flux rates were obtained with symmetrical minerals of narrow particle size distribution, such as limestone, whereas superior permeate quality was obtained with highly irregular silicate flake particles. Groves et al. (7) investigated the use of zirconium as a dynamic membrane in treating industrial effluents from polymer manufacturing and viscose/polyester dyeing factories. They reported that dynamic membranes produced high flux values and had the ability to treat industrial effluents.

The most important recent developments in systems for critical applications involve surface modification of membranes. These developments optimize membrane performance in terms of process efficiency and membrane lifetime without compromising the security of the absolute removal of the final contaminants in any way. Orchard (8) reported that the material from which surface-modified membranes are manufactured has to be selected for its capacity to form a physically and chemically stable structure with the requisite removal ability.

The progressive decline of flux with time cannot be avoided, and eventually the flux becomes uneconomically low. Consequently, some type of cleaning or regeneration of the membrane must be carried out. The cleaning process and its frequency depend on the filtered product and on the chemical resistance of the membrane. Most cleaning procedures are a combination of hydraulic and chemical cleaning.

## Fouling Mechanisms

Fouling mechanisms were divided into three categories on the basis of dynamic membrane formation by Tanny (9). Class I dynamic membranes are formed when suspensions in which the particles have a particle size greater than the pore size of the membrane are filtered. This phenomenon is known as concentration polarization.

Class II dynamic membranes are created when dilute suspensions of colloidal particles with a particle size much smaller than the pore size of the membrane are filtered. In this case the flux decline mechanism was found to behave

according to an internal pore clogging phenomenon rather than by cake buildup on the membrane surface. Visvanathan and Ben Aim (10) and other investigators (11–14) reported similar results. All investigators reported the following fouling model which represents the decrease in permeate volume:

$$\frac{t}{V} = \frac{1}{Q_0} + \frac{k_1 t}{2}$$

where $V$ is the permeate volume, $t$ is the filtration time, $Q_0$ is the initial flux rate, and $k_1$ is the filtration constant.

After some time the colloidal particles will be brought up to the membrane surface and the flux behavior will proceed in accordance with the following classical cake filtration model (15):

$$\frac{t}{V} = \frac{1}{K_1}(V - 2V_f)$$

where $V_f$ is the volume of permeate which produces a hydraulic resistance equal to that of the membrane, and $K_1$ is the cake filtration constant. A different form of the cake filtration model was reported by Visvanathan and Ben Aim (10):

$$\frac{t}{V} = \frac{1}{Q_0} + \frac{K_1 V}{2}$$

Al-Malack and Anderson (16) investigated the formation of dynamic membranes with crossflow microfiltration. They concluded that dynamic membrane formation obeys the standard law of filtration in the first few minutes of membrane formation (15 minutes). As time passes, the dynamic membrane formation was found to proceed according to the classical cake filtration model. Moreover, Akay et al. (17) investigated the removal of phosphate from water by red mud using crossflow microfiltration. They evaluated the specific cake resistance in crossflow microfiltration as a function of phosphate concentration by using the cake filtration model. Tanaka et al. (18) investigated the characteristics in crossflow microfiltration using different yeast suspensions. They reported that the experimental steady-state flux agreed well with the those calculated by the following equation, which is used in dead-end filtration:

$$J = \frac{\Delta P}{\mu(R_m + R_c)}$$

where $J$ is the permeate flux, $\Delta P$ is the pressure difference across the membrane, $\mu$ is the liquid viscosity, $R_m$ is the membrane hydraulic resistance, and $R_c$ is the cake hydraulic resistance.

Class III dynamic membranes are formed when filtering polymers or polyelectrolyte molecules of equal size to the membrane size.

Based on the above discussion, the main objective of this study was to investigate the feasibility of exploiting the phenomenon of dynamic membrane formation with crossflow microfiltration by using various chemical species and to compare the results with those obtained with $MnO_2$. Calcium carbonate ($CaCO_3$), ferric chloride ($FeCl_3$), and sodium aluminate ($NaAlO_2$) were used in this investigation. The formation of dynamic membranes was investigated at different chemical concentrations. The fouling mechanisms of the various dynamic membranes were investigated.

## MATERIALS AND METHODS

The setup used in this study is shown in Fig. 1. The membrane was made of multifilament polyester yarn with an internal diameter of 25 mm. Table 1 shows the general characteristics of the membrane.



V1 - V6 = VALVES
1 = HEADER TANK
3 = CIRCULATION PUMP
5 = INLET PRESSURE GAUGE
7 = OUTLET PRESSURE GAUGE

FT = FEED TANK
2 = CIRCULATION TANK
4 = FLOW METER
6 = AIR INJECTION
8 = PERMEATE TANK

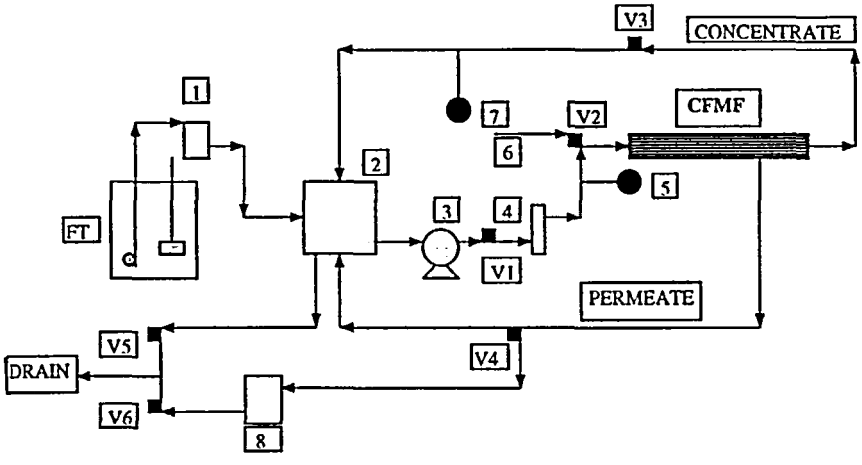


FIG. 1 Flow diagram of the process.

TABLE 1
Characteristics of the Woven Fabric

| | |
|---|---|
| Configuration | Tubular |
| Material | Polyester |
| Pore size | 20 to 40 μm |
| Radius | 1.25 cm (0.5 inch) |
| Length | 4 × 0.98 m |
| Cross-sectional area | 4.597 $cm^2$ |
| Total surface area | 0.295 $m^2$ |
| Wall thickness | 0.34–0.375 mm |
| Hydraulic resistance | $2.7 \times 10^6$ (1/m) |
| pH resistance range | 2–14 |



Secondary effluent from an activated sludge wastewater treatment plant was used throughout the research period. The wastewater has the typical characteristics shown in Table 2.

Suspensions of $CaCO_3$ were circulated for 30 minutes, using the circulation tank, in order to form the dynamic membrane. Two grades of $CaCO_3$, light and heavy, were used to form dynamic membranes. As supplied by the manufacturer (Merck Ltd), the pore size of the light grade ranges between 0.5 to 15 μm; the pore size is more than 5 μm for the heavy grade. Additionally, the bulk density for light and heavy grades are 25 to 30 and 50 to 60 g/mL, respectively.

In the case of $FeCl_3$ and $NaAlO_2$, the coagulants were added to either tap water or the wastewater to form flocs in the circulation tank. The pH value

TABLE 2
Wastewater Characteristics

| Constituent | Value |
|---|---|
| Turbidity (NTU) | 22 |
| pH | 7.45 |
| Density (g/L) | 1001.84 |
| Viscosity (cpu) | 1.07 |
| Alkalinity (mg/L) | 300 |
| Chlorides (mg/L) | 3720 |
| Sulfates (mg/L) | 640 |
| Suspended solids (mg/L) | 66 |
| COD (mg/L) | 130 |
| BOD (mg/L) | 20 |
| TOC (mg/L) | 86 |

was adjusted to about 7 using sodium hydroxide (NaOH). The circulation tank contents were circulated for 10 to 15 minutes to form the dynamic membrane.

The permeation rate (flux) and the inlet and outlet pressures were measured. The turbidity of the permeate was determined using Hach turbidometer.

Routine cleaning was carried out at the end of each run using brushes on the outside surface of the woven fabric.

## RESULT AND DISCUSSION

The following paragraphs discuss the results obtained on dynamic membranes formed from $CaCO_3$, $FeCl_3$, and $NaAlO_2$.

### Calcium Carbonate ($CaCO_3$)

Figure 2(a) shows the permeate flux with respect to running time of a set of runs where the light grade of $CaCO_3$ was used in the dynamic membrane formation. The figure shows that when $MnO_2$ was used in forming the dynamic membrane, the permeate flux started with a value of 660 $L/m^2 \cdot h$ and decreased to 94 $L/m^2 \cdot h$ at the end of the run (300 minutes). Due to relatively high initial flux values, the time needed to form the dynamic membrane was extended from 15 to 30 minutes when light $CaCO_3$ was used. The figure clearly shows that as the amount of light $CaCO_3$, used in the dynamic membrane formation was increased, the flux stabilized at higher values. Using 1250 mg/L of light $CaCO_3$ resulted in a relatively lower initial flux value (590 $L/m^2 \cdot h$). The flux at the end of the run stabilized at 90 $L/m^2 \cdot h$. The results show that as the concentration of $CaCO_3$ increased, the flux stabilized at higher values. It is clear that a large amount of $CaCO_3$ and a long circulation period were needed in order to form a dynamic membrane which produced results similar to those produced by the $MnO_2$ dynamic membrane. This can be attributed to the hydrophilic/hydrophobic nature of both of the dynamic membrane ($CaCO_3$) and the primary membrane (polyester). Both membranes are made of hydrophobic materials, which results in the creation of repulsive forces between the materials.

Figure 2(b) shows the permeate turbidity with respect to time. When $MnO_2$ was used as the dynamic membrane, the permeate turbidity started with a value of 0.24 NTU and stabilized around 0.21 NTU after 20 minutes of running time. The figure also shows that increasing the concentration of light grade $CaCO_3$ used in forming the dynamic membrane results in improving the permeate quality. For instance, using 1250 mg/L of $CaCO_3$ resulted in an initial permeate turbidity of 0.5 NTU which improved until it reached a value of 0.23 NTU at the end of the run.

The results on permeate flux and turbidity show that increasing the quantity of light grade $CaCO_3$ used in forming the dynamic membrane results in ex-

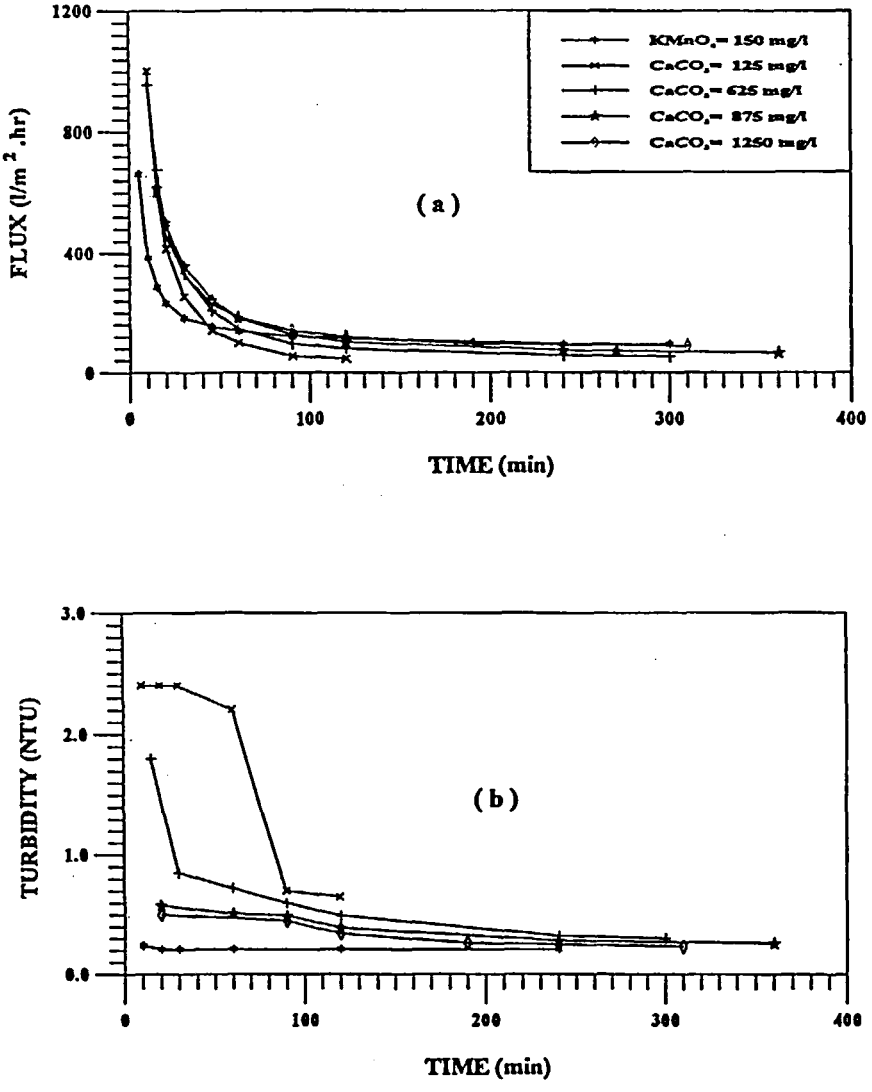


FIG. 2 Permeate flux and turbidity vs time when using light $CaCO_3$ as a dynamic membrane.

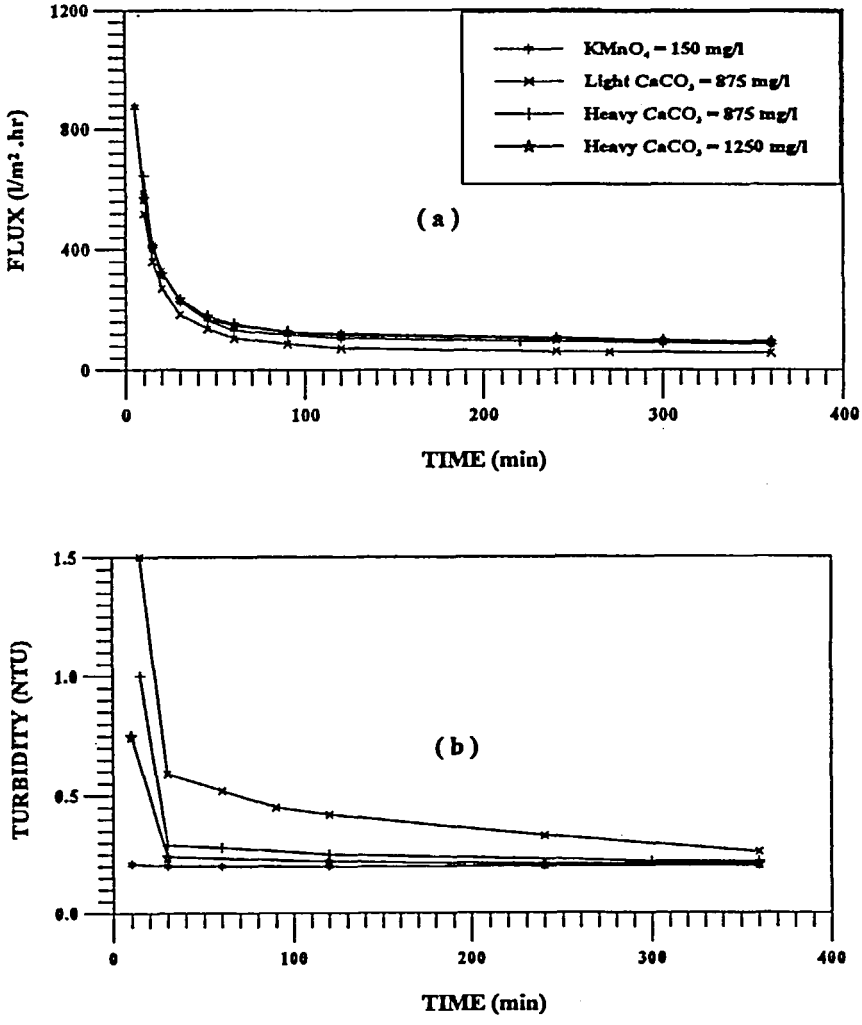


FIG. 3 Permeate flux and turbidity vs time using various materials for dynamic membrane formation.

tending the running time and the production of a better permeate quality. This can be attributed to narrowing of the pore size of the primary membrane.

Figure 3(a) shows the permeate flux values with respect to time for a set of runs where $MnO_2$ and light and heavy grade $CaCO_3$ were used in forming the dynamic membrane. The use of $MnO_2$ produced an initial flux value of 880 L/m$^2$·h which stabilized at 95 L/m$^2$·h after 360 minutes of running time. When 875 mg/L of light $CaCO_3$ was used, the permeate flux started at 520 L/m$^2$·h and reached 56 L/m$^2$·h by the end of the run. In comparison, when 875 mg/L of heavy grade $CaCO_3$ was used, the permeate flux started with a value of 650 L/m$^2$·h and after 360 minutes of running time decreased to 85 L/m$^2$·h. These results show that heavy grade $CaCO_3$ produces much higher flux values than does the light grade. This can be attributed to the grain size of heavy grade $CaCO_3$ which may have influenced the flux decay behavior. No information was provided by the manufacturer on the grain sizes of light and heavy grades of $CaCO_3$, but information on their pore sizes suggests that the grain size of the heavy grade is larger than that of the light grade.

The permeate turbidity with respect to running time is shown in Fig. 3(b), which shows that the best permeate quality was obtained with $MnO_2$ when used as a dynamic membrane (0.20 NTU). The figure also shows that the permeate quality improved with an increase in the concentration of heavy grade $CaCO_3$ and that the use of 1250 mg/L produced a low turbidity value (0.21 NTU) at the end of the run. The figure shows that the use of heavy grade $CaCO_3$ produced better permeate quality than the light grade.



## Ferric Chloride ($FeCl_3$)

Figure 4(a) shows the permeate flux with respect to running time for a set of runs where ferric chloride was added to tap water for the purpose of dynamic membrane formation. The figure also compares such dynamic membranes with the $MnO_2$ dynamic membrane. When $MnO_2$ was used, the permeate flux started with a value of 660 L/m$^2$·h and stabilized at 88 L/m$^2$·h after 360 minutes of running time. When 60 mg/L of $FeCl_3$ was used in forming the dynamic membrane, the initial flux value was around 470 L/m$^2$·h and stabilized at 70 L/m$^2$·h after 360 minutes. It was noticed that the flux decay rate was slower in the first 90 minutes than when $MnO_2$ was used as the dynamic membrane. This is attributed to the flocculation taking place inside the circulation tank due to the availability of $FeCl_3$. After 90 minutes the flux started to decline at a higher rate than with $MnO_2$. The figure clearly shows that increasing the concentration of $FeCl_3$ results in decreasing the initial flux values, which is attributed to the formation of flocs. Floc formation becomes denser with an increase in the concentration of $FeCl_3$. The effect on the

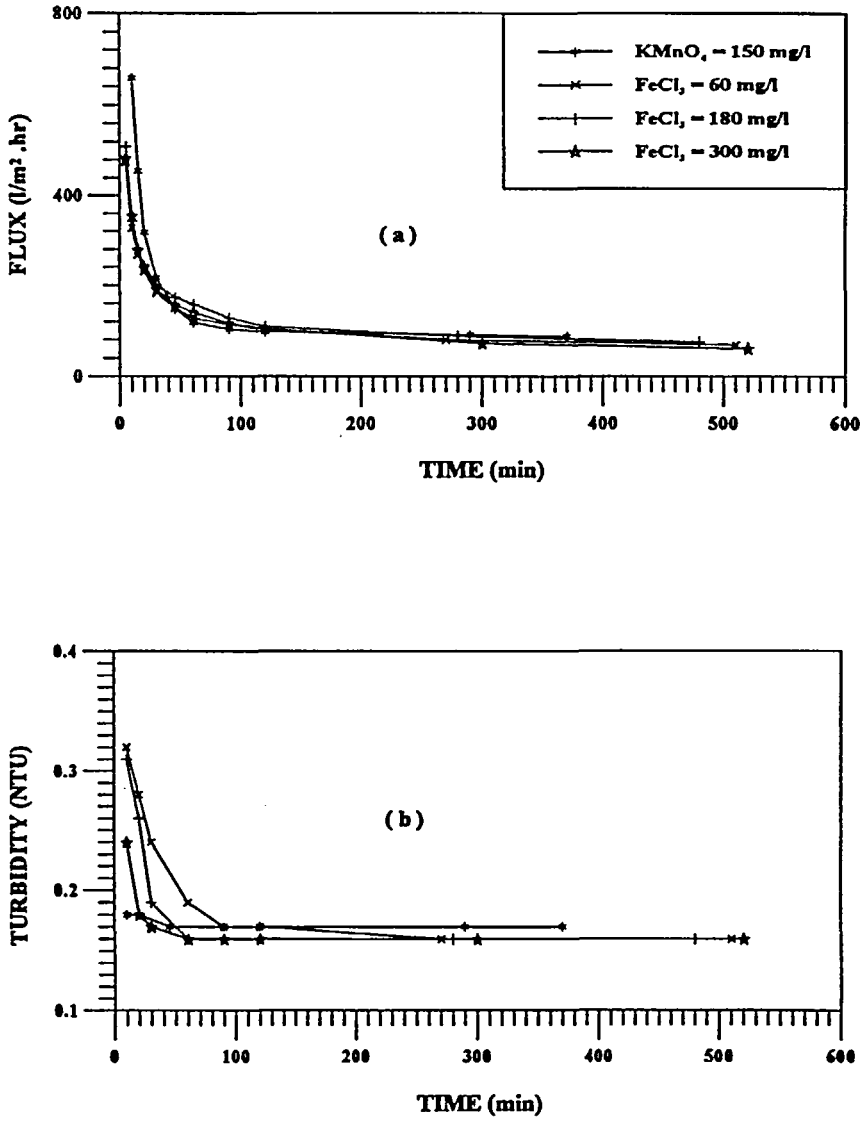


FIG. 4 Permeate flux and turbidity vs time using $FeCl_3$ as a dynamic membrane when mixed with tap water.

stabilized flux values of increasing the concentration of $FeCl_3$ was not significant.

The permeate turbidity is shown in Fig. 4(b). The figure shows that the $MnO_2$ dynamic membrane produced a permeate turbidity of 0.17 NTU. When 60 mg/L of $FeCl_3$ were used, the initial turbidity value was greater (0.32 NTU) than that obtained with $MnO_2$. This turbidity decreased with time and reached a value of 0.16 NTU by the end of the run. The figure also shows that as the concentration of $FeCl_3$ increases, the permeate initial turbidity decreases, while the final turbidity was the same for all the runs. This difference in initial permeate turbidity can be attributed to the amount of precipitating materials on the inside surface of the woven fabric.

When lower concentrations of $FeCl_3$ (60–180 mg/L) were mixed with the wastewater in order to form the dynamic membrane, the filter clogged very fast during the formation of the dynamic membrane, and the turbidity did not improve significantly. In all cases the floc formation was not visually apparent, which could be why the filter clogged rapidly. It seems that the amount of $FeCl_3$ was not enough to flocculate the solids in the wastewater, which resulted in clogging the membrane in a short time.

When 300 mg/L of $FeCl_3$ was mixed with the wastewater, the situation improved. Figure 5(a) shows that the initial permeate flux was about 220 L/$m^2$·h and decreased to a value of around 50 L/$m^2$·h within 300 minutes of running time. Using the $MnO_2$ dynamic membrane, the flux started at 370 L/$m^2$·h and stabilized at 80 L/$m^2$·h after 360 minutes. The figure also shows that by increasing the concentration of $FeCl_3$ used in the dynamic membrane formation to 480 mg/L, the initial permeate flux increased to 430 L/$m^2$·h and stabilized at 60 L/$m^2$·h. A further increase in the $FeCl_3$ concentration to 600 mg/L did not improve the situation significantly.

Figure 5(b) shows the permeate turbidity with respect to running time. When $MnO_2$ was used as the dynamic membrane, the turbidity began with 0.22 NTU and started to stabilize at around 0.17 NTU after 60 minutes. The figure shows that as the concentration of $FeCl_3$ was increased, the initial permeate turbidity decreased. The turbidity stabilized around 0.19 NTU for all cases. This can be attributed to narrowing of the pore size of the primary membrane.

## Sodium Aluminate ($NaAlO_2$)

Mixing $NaAlO_2$ with either tap water or wastewater for the purpose of dynamic membrane formation was investigated. When tap water was used, the membraning flux at the end of the dynamic membrane formation was relatively high (5360 L/$m^2$·h) compared to that when wastewater was used (200 L/$m^2$·h). This can be attributed to the solid particles in the wastewater.

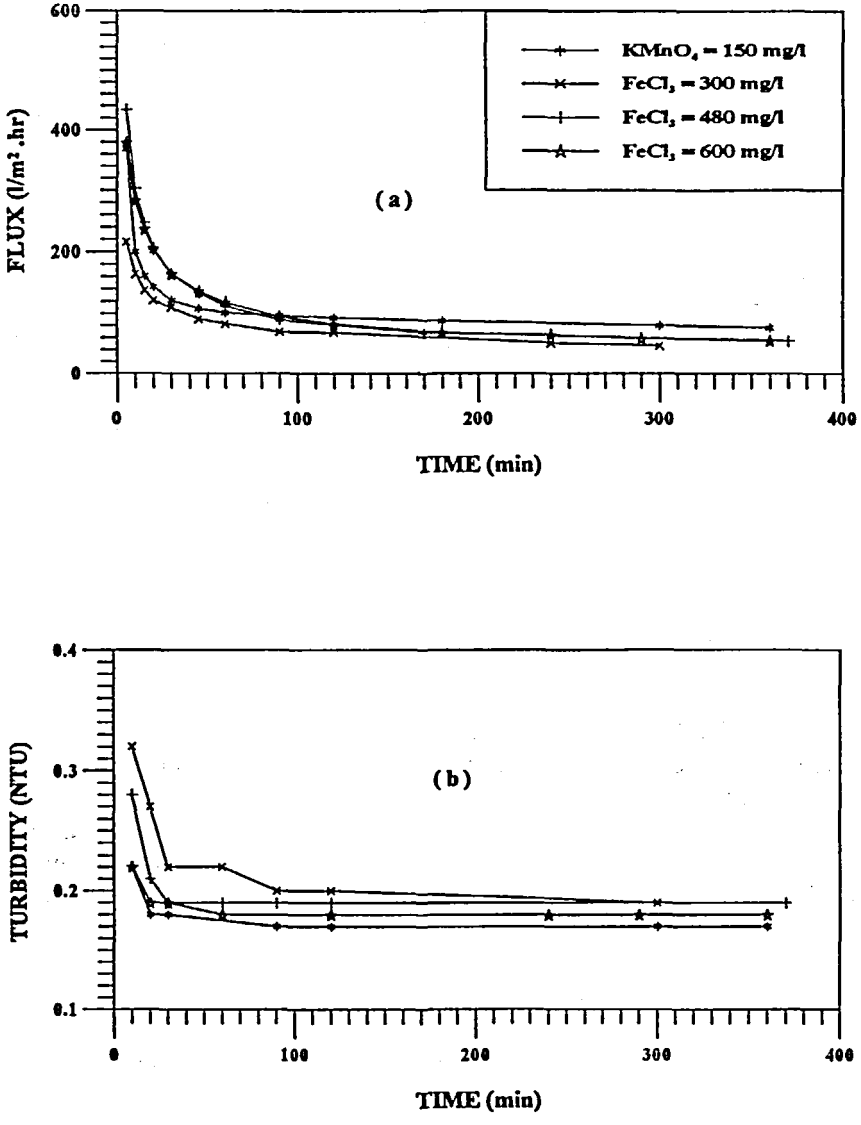


FIG. 5 Permeate flux and turbidity vs time using $FeCl_3$ as a dynamic membrane when mixed with wastewater.

Figure 6(a) shows that when tap water was used in forming the dynamic membrane, the flux decreased sharply in the first 5 minutes (i.e., down to 380 $L/m^2 \cdot h$). This suggests that the concentration of $NaAlO_2$ used in forming the dynamic membrane was not enough to cover the surface of the primary membrane. Another possible reason, which depends totally on visual observation, is the floc fragility. The flocs formed in this case were very fluffy and appeared not to sustain high pressures. The permeate flux was about the same for both cases in the later stages. Figure 6(b) shows that when tap water was used, the initial permeate turbidity was higher (0.27 NTU) than when wastewater was used (0.22 NTU). The turbidity stabilized around the same value (0.18 NTU) in both cases. The higher initial turbidity value can be attributed to the same reasons as are given above.

Figure 7(a) shows the permeate flux with respect to running time. When the $MnO_2$ dynamic membrane was used, the flux started at 530 $L/m^2 \cdot h$ and stabilized at around 74 $L/m^2 \cdot h$. When 250 mg/L of $NaAlO_2$ was used, the flux started with a lower value (380 $L/m^2 \cdot h$). The reason for that, as discussed before, could be the concentration of $NaAlO_2$ used in forming the dynamic membrane. The results show that by increasing the concentration of $NaAlO_2$ used in forming the dynamic membrane, the permeate flux increases up to a certain value, beyond which no improvement occurs. This can be attributed to the floc size because different $NaAlO_2$ concentrations produce different sized flocs. The use of 750 mg/L $NaAlO_2$ produced the optimum floc size for forming the dynamic membrane.

Figure 7(b) shows permeate turbidity with respect to running time. With $MnO_2$, the turbidity did not change significantly. It started at 0.20 NTU and stabilized at 0.18 NTU. The figure shows that increasing the $NaAlO_2$ concentration decreases the permeate turbidity; the lowest turbidity was obtained with 750 mg/L of $NaAlO_2$ (0.16 NTU). The figure shows that turbidity values were almost stable with all $NaAlO_2$ concentrations.

## Fouling Mechanisms

The objective of this section is to evaluate the mechanism by which the dynamic membrane material is being fouled when treating wastewater. The standard law of filtration and the classical cake filtration models will be used.

Figure 8(a) shows that the light and heavy grades of $CaCO_3$ behave in a similar way. In the beginning the fouling mechanism of both dynamic membranes proceeded in accordance with the standard law of filtration. This is attributed to the infiltration of colloidal particles into the pores of the dynamic membranes. Light grade $CaCO_3$ produced the following empirical model based on Fig. 8(a):

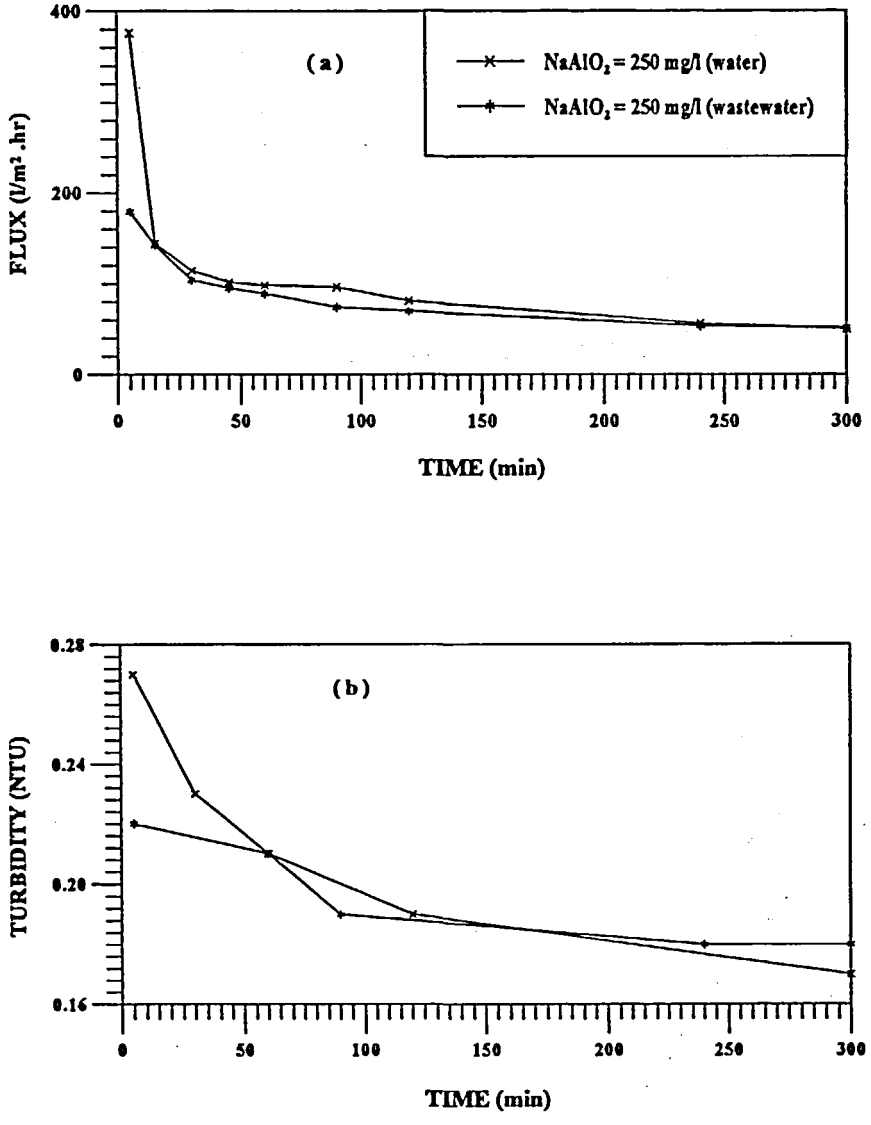


FIG. 6 Permeate flux and turbidity vs time using $NaAlO_2$ as a dynamic membrane mixed with water and wastewater.

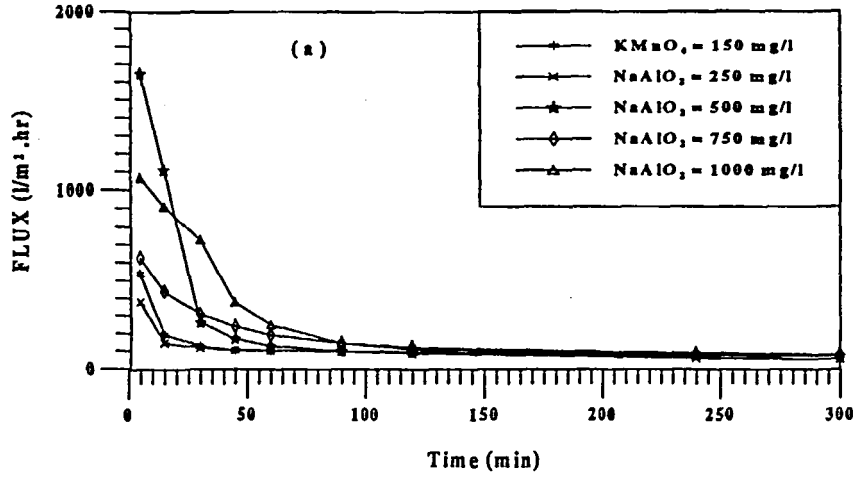


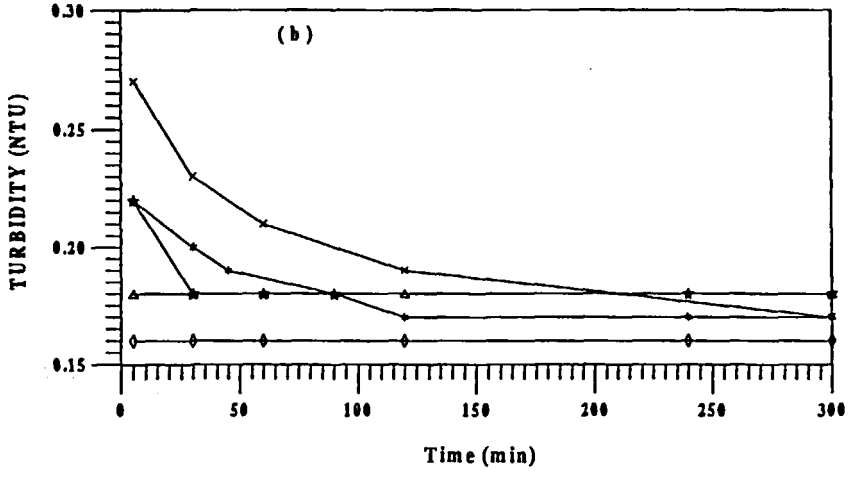


FIG. 7 Permeate flux and turbidity vs time using $NaAlO_2$ as a dynamic membrane when mixed with tap water.

$$t/V = 0.00274t + 0.017$$

with $k_1 = 0.00555$/L and $Q_0 = 60$ L/min. The heavy grade $CaCO_3$ dynamic membrane produced the following empirical model:

$$t/V = 0.0038t + 0.0204$$

with $k_1 = 0.0076$/L and $Q_0 = 50$ L/min.

Figure 8(b) shows that after 1 hour of running time the fouling mechanism of the dynamic membranes proceeded according to the cake filtration model. With light grade $CaCO_3$ the following empirical model was obtained:

$$t/V = 0.0038V - 1.10$$

with $K = 263$ L$^2$/min and $V_f = 145$ L.

The heavy grade $CaCO_3$ dynamic membrane was represented by the following empirical model:

$$t/V = 0.004V - 0.714$$

with $K = 250$ L$^2$/min and $V_f = 90$ L.

The results of Figs. 8(a) and 8(b) show that a dynamic membrane created from the constituents in the wastewater forms on top of the $CaCO_3$ dynamic membrane.

The fouling mechanism of the $NaAlO_2$ dynamic membrane was found to be similar to that of $CaCO_3$. Figure 8(a) shows that the standard law of filtration dominates the process in the early stages of treatment. The following empirical model was obtained:

$$t/V = 0.0049t + 0.273$$

with $k_1 = 0.0098$/L and $Q_0 = 3.7$ L/min.

Figure 8(b) shows that in later stages of treatment the fouling mechanism of the $NaAlO_2$ dynamic membrane proceeds in accordance with the cake filtration model. The empirical model obtained was

$$\frac{t}{V} = 0.0059V - 0.0798$$

with $K = 169$ L$^2$/min and $V_f = 6.8$ L.

The ferric chloride dynamic membrane was seen to behave in a completely different way. Figure 9(a) shows that in the beginning the $FeCl_3$ dynamic membrane fouls in accordance with the cake filtration model as reported by Visvanathan and Ben Aim (10). The following empirical model was obtained when water was used in the dynamic membrane formation:

$$t/V = 0.0112V + 0.229$$

with $K_1 = 0.0224$ min/L$^2$ and $Q_0 = 4.37$ L/min.

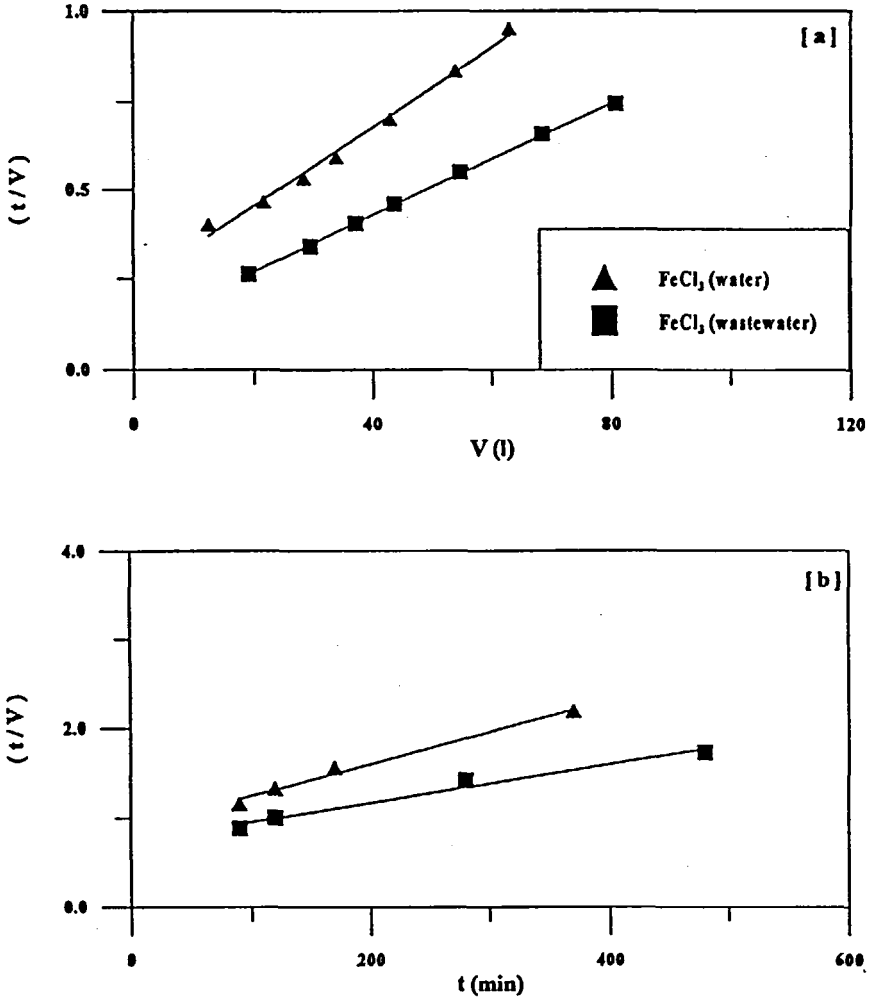


FIG. 9 Relationship between (a) ($t/v$) and $V$ and between (b) ($t/V$) and $t$ for $FeCl_3$.

When wastewater was used in forming the dynamic membrane, the empirical model obtained was

$$t/V = 0.00796V + 0.109$$

with $K_1 = 0.0159$ min/L$^2$ and $Q_0 = 9.17$ L/min.

Figure 9(b) shows that the fouling mechanism of the $FeCl_3$ dynamic membrane proceeds according to the standard law of filtration in the later stages of treatment. When water was used in forming the dynamic membrane, the following empirical model was obtained:

$$\frac{t}{V} = 0.00356t + 0.891$$

with $k_1 = 0.00712$/L and $Q_0 = 1.12$ L/min.

When wastewater was used in forming the dynamic membrane, the empirical model obtained was

$$t/V = 0.00215t + 0.74$$

with $k_1 = 0.0043$/L and $Q_0 = 1.35$ L/min.

The reason for such different behaviors can be attributed to the fact that when $FeCl_3$ is used in forming the dynamic membrane, the formation of very dense flocs takes place when wastewater is introduced to the circulation tank for treatment. This might result in precipitating a layer of the flocculated wastewater on top of the dynamic membrane in the early stages of treatment. As time passes, and when no more floc formation is taking place, colloidal particles in the wastewater start to infiltrate both the precipitated layer and the dynamic membrane.



## SUMMARY AND CONCLUSION

The feasibility of utilizing the phenomenon of dynamic membrane formation with crossflow microfiltration in treating secondary effluent was investigated. Using $CaCO_3$, the results showed that large quantities (1250 mg/L) and long circulation periods (30 minutes) are needed to form a dynamic membrane which produces reliable results on permeate flux and turbidity. Ferric chloride and sodium aluminate dynamic membranes produced the best results when they were mixed with tap water during the formation of the dynamic membrane. Mixing $FeCl_3$ and $NaAlO_2$ with wastewater to form the dynamic membrane clogged the membrane very fast. The results on fouling mechanisms showed that $CaCO_3$ and $NaAlO_2$ dynamic membranes were initially fouled in accordance with the standard law of filtration, As time passes, the fouling mechanism of $CaCO_3$ and $NaAlO_2$ dynamic membranes was seen to proceed according to the cake filtration model. The fouling mechanism of the ferric chloride dynamic membrane was seen to proceed in accordance

with the cake filtration model in the early stages, followed by the standard law of filtration. This was attributed to the heavy and dense floc formation seen at the time of wastewater treatment.

## ACKNOWLEDGMENT

The authors thank King Fahd University of Petroleum & Minerals, (Dhahran, Saudi Arabia) for the support provided during manuscript preparation.

## REFERENCES

1. J. Murkes, "Fundamentals of Crossflow Filtration," *Sep. Purif. Methods*, *19*(1), 1 (1990).
2. Milisic and Bersillon, "Anti-Fouling Techniques in Crossflow Microfiltration," *Filtr. Sep.*, *23*(6), 347 (1986).
3. M. Mulder, *Basic Principles of Membrane Technology*, Kluwer Academic Publishers, Dordrecht, The Netherlands, 1991.
4. S. Ripperger, "Microfiltration," in *Water, Wastewater and Sludge Filtration* (S. Vigneswaran and R. Ben Aim, Eds.), CRC Press, Boca Raton, FL, 1989.
5. M. H. Al-Malack and G. K. Anderson, "Crossflow Microfiltration with Dynamic Membranes," *Water Res.*, *31*(8), 1969 (1997).
6. R. G. Holdich and R. G. Boston, "Microfiltration Using a Dynamically Formed Membrane," *Filtr. Sep.*, *27*(3), 192 (1990).
7. G. R. Groves, C. A. Buckley, J. M. Cox, A. Kirk, and M. J. Simpson, "The Treatment of Industrial Effluents by Dynamic Membrane Technology," *Chem*, *10*(4), 350 (1984).
8. A. C. J. Orchard, *Recent Developments in Membranes for Critical Filtration Applications.* Paper Presented at the International Technical Conference on Membrane Separation Processes, Brighton, UK, May 24–26, 1989.
9. G. B. Tanny, "Dynamic Membranes in Ultrafiltration and Reverse Osmosis," *Sep. Purif. Methods*, *7*(2), 183 (1978).
10. C. Visvanathan and R. Ben Aim, "Studies on Colloidal Membrane Fouling Mechanisms in Crossflow Microfiltration," *J. Membr. Sci.*, *45*(1/2), 3 (1989).
11. H. P. Grace, "Structure and Performance of Filter Media," *AICh J.*, 2, 307 (1956).
12. G. B. Tanny, D. K. Strong, W. G. Presswood, and T. H. Meltzert. "The Adsorptive Retention of *Pseudomonas diminuta* by Membrane Filters," *J. Parenter Drug Assoc.*, *33*, 40 (1979).
13. J. V. Hermia, "Constant Pressure Blocking Filtration Laws—Application to Power-Law Non-Newtonian Fluids," *Trans. Inst. Chem. Eng.*, *60*, 183 (1982).
14. C. Cabassud, "Microfiltration tangentielle et separation de biomass," Doctoral Thesis, ENSIGC, INTP, Toulouse, France.
15. J. Murkes and C. G. Carlsson, *Crossflow Filtration.* Wiley, Chichester, UK, 1988
16. M. H. Al-Malack and G. K. Anderson, "Formation of Dynamic Membranes with Crossflow Microfiltration," *J. Membr. Sci.*, *112*, 287 (1996).
17. G. Akay, B. Keskinler, A. Cakici, and U. Danis, "Phosphate Removal from Water by Red Mud Using Crossflow Microfiltration," *Water Res.*, *32*(3), 717 (1998).
18. T. Tanaka, S. Tsuneyoshi, W. Kitazawa, and K. Nakanishi, "Characteristics in Crossflow Filtration Using Different Yeast Suspension," *Sep. Sci. Technol.*, *32*(11), 1885 (1997).

*Received by editor August 21, 1997*
*Revision received March 1998*